

# Phase-Optimized Peristaltic Pumping by Integrated Microfluidic Logic

## Supplementary Materials

Erik M. Werner, Benjamin Lam, and Elliot E. Hui

### Contents:

Figure S1: Rapid prototyping process

Figure S2: Control of channel depth with a CO<sub>2</sub> laser

Figure S3: Working principle of an oscillator pump

Figure S4: Mixing performance quantification

Figure S5: Series vs parallel pump configuration

Figure S6: Valve deflection measurement

Figure S7: Experimental setup

Table S1: Iterative design progression

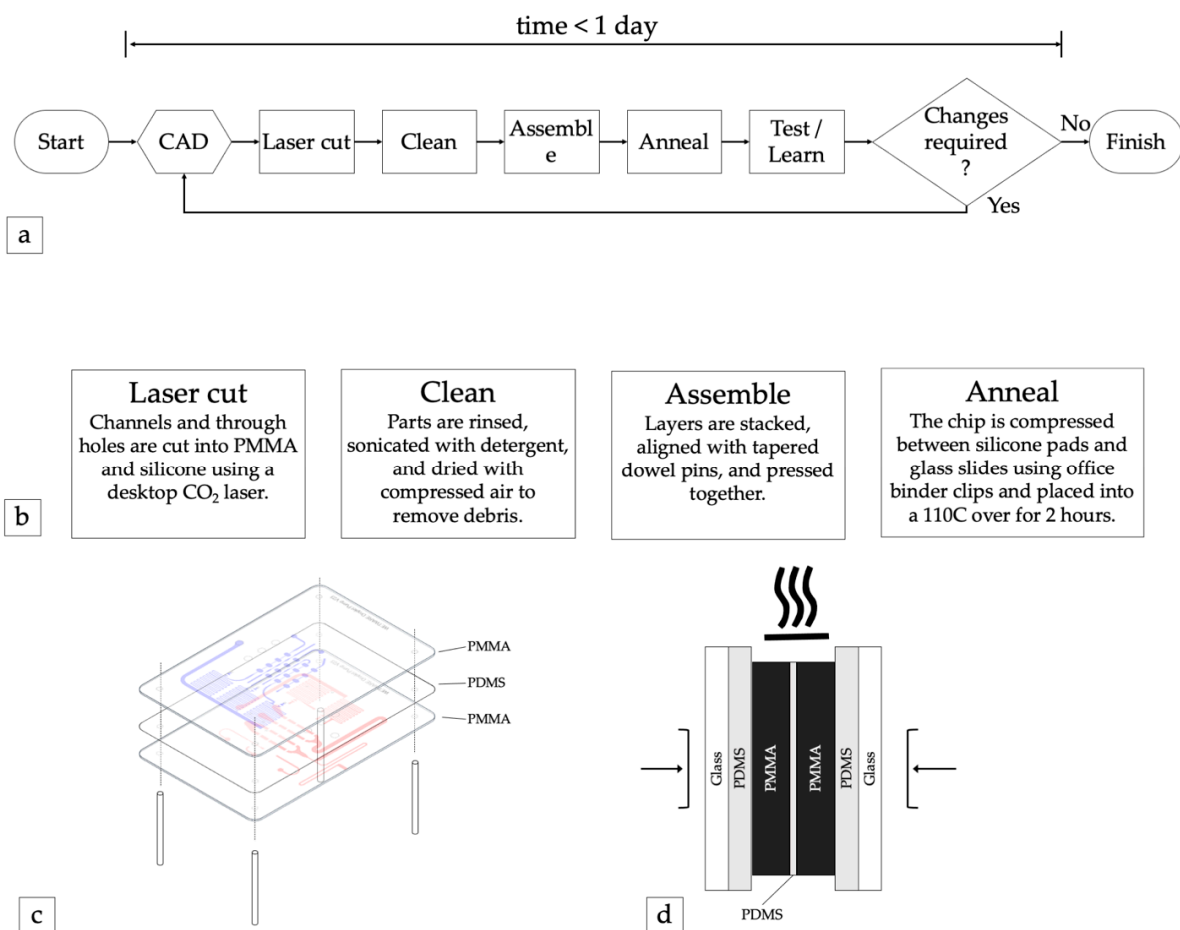
Video S1: Steady state oscillator pump droplet generation from 50 kPa constant vacuum source

Video S2: Electricity free droplet generation from 60 mL syringe pull

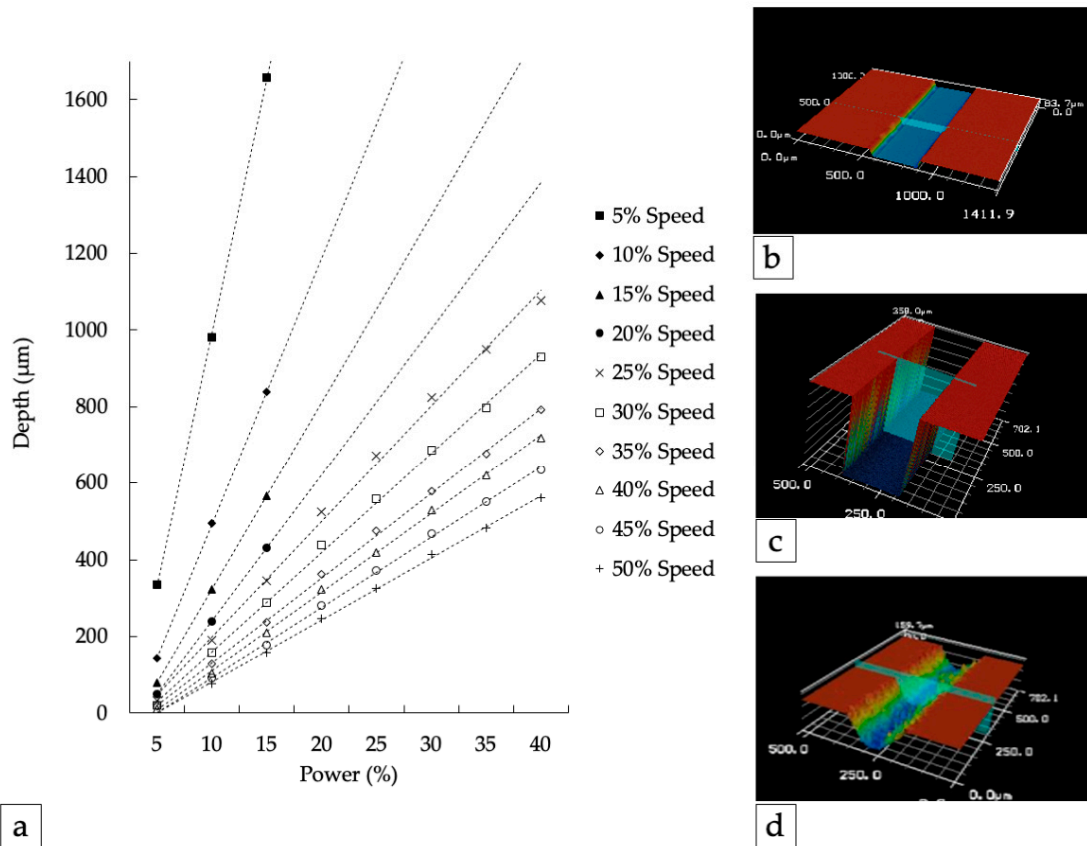
Video S3: Droplet generator response time

Calculation S1: Hydraulic resistance calculations

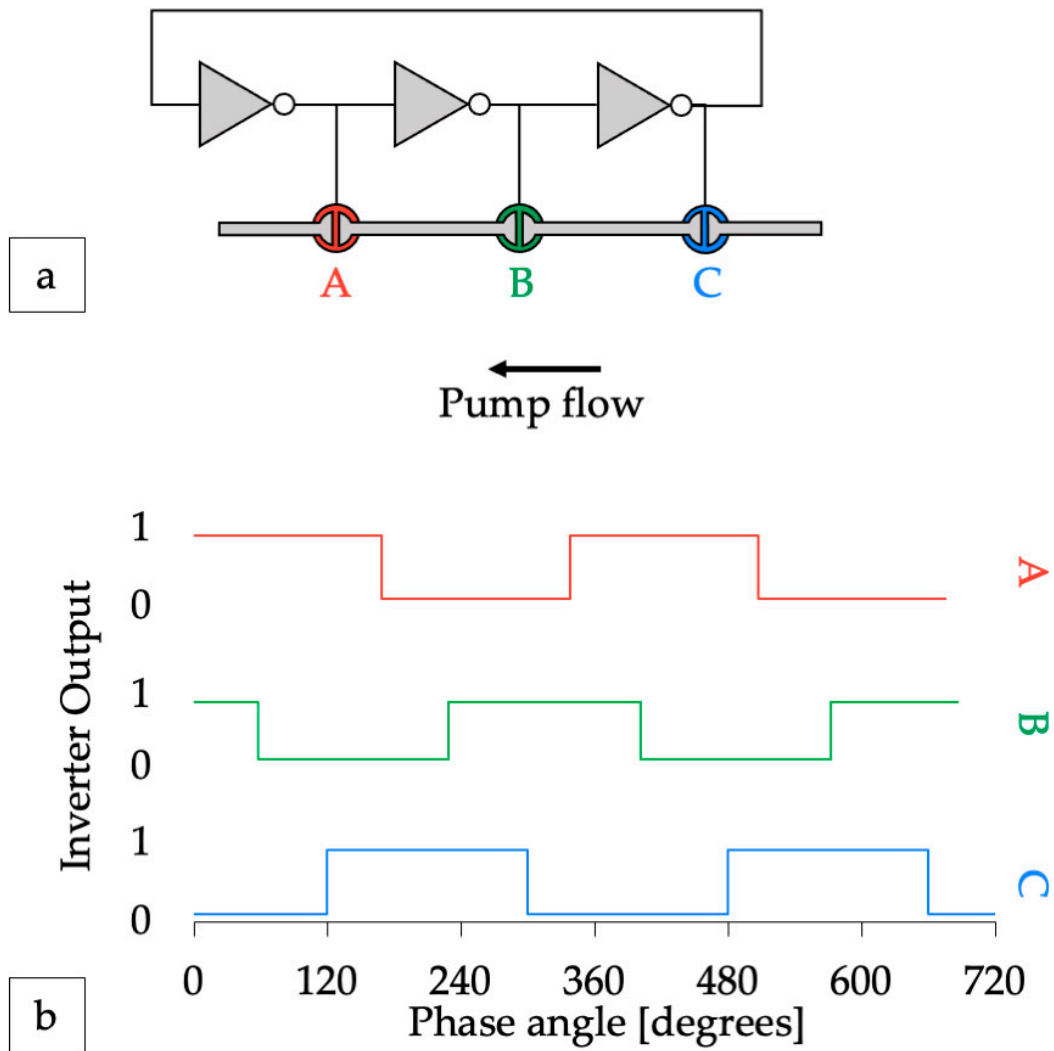
Calculation S2: Capillary number calculations



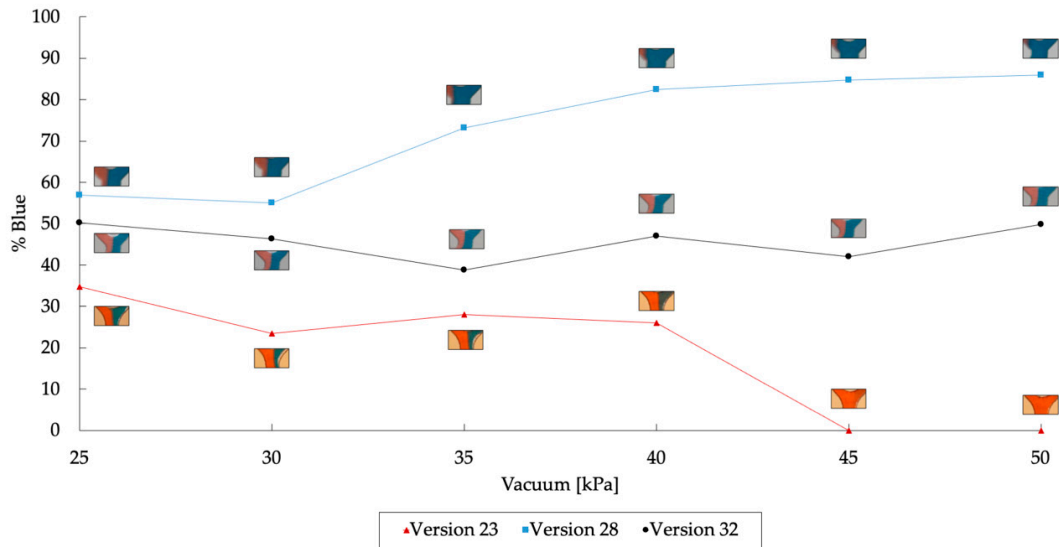
**Figure S1:** Rapid prototyping process for microfluidic digital logic circuits. **(a)** Design, build, test, learn process enabled through rapid prototyping **(b)** Fabrication method details **(c)** Alignment and assembly of device layers **(d)** Side view of assembled device during bonding. Devices were clamped between additional pieces of PDMS and glass slides for bonding.



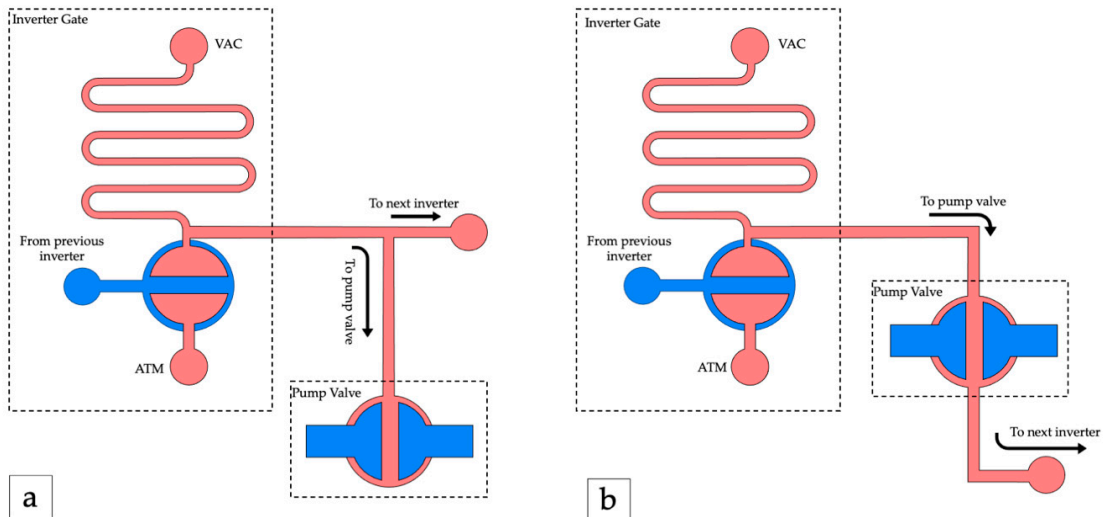
**Figure S2:** Depth control CO<sub>2</sub> of laser-fabricated microchannels. **(a)** Engraving depth vs laser power. Data are presented as the average depth at the center of the channel. Dotted lines represent linear fits. Speed values are presented as a percent of the maximum raster speed of the laser (40 in/sec). Power values are presented as a percent of the maximum power of the laser (60W). **(b-d)** Surface profiles of channels produced by wet etching (250  $\mu\text{m}$  width x 83  $\mu\text{m}$  height), CNC micro milling (200  $\mu\text{m}$  x 350  $\mu\text{m}$ ), and CO<sub>2</sub> laser engraving (200  $\mu\text{m}$  x 100  $\mu\text{m}$ ).



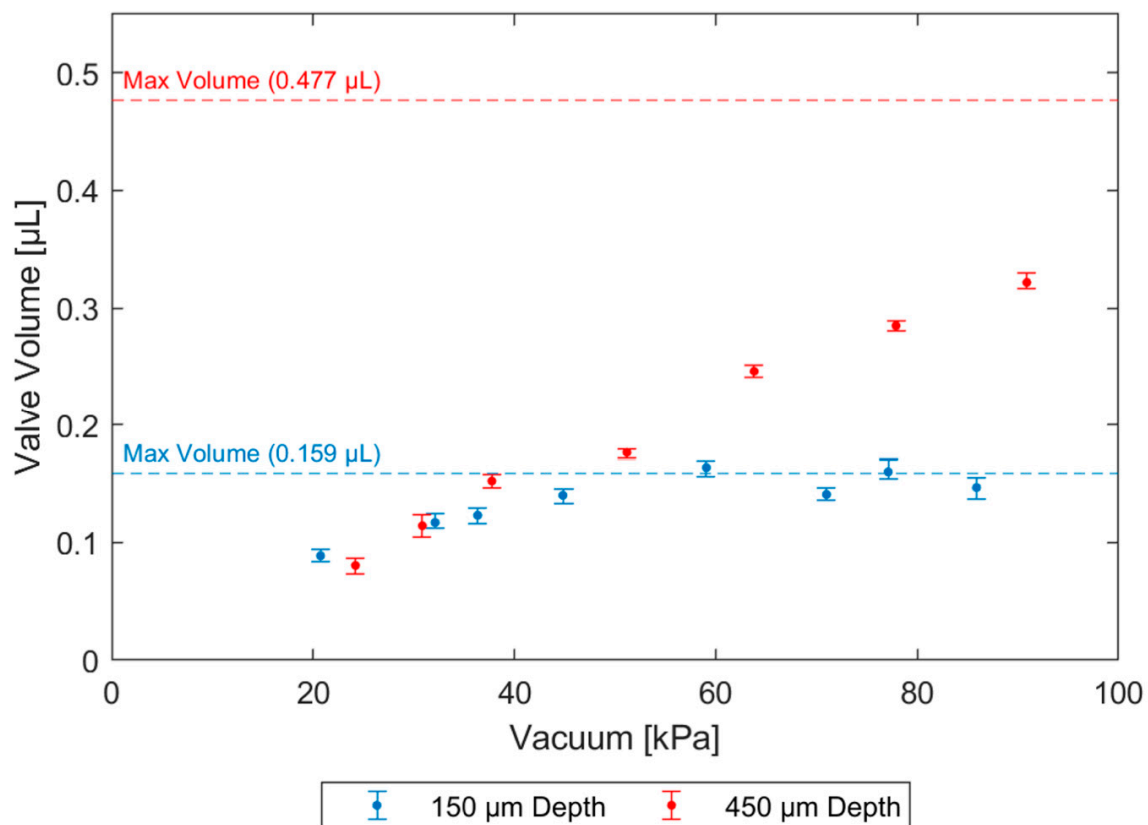
**Figure S3:** Oscillator pump working principle. **(a)** Each node of a three-inverter ring oscillator is connected to pump valves (A,B,C). **(b)** The ideal waveform output from the ring oscillator generates a pattern that produces peristaltic pumping.



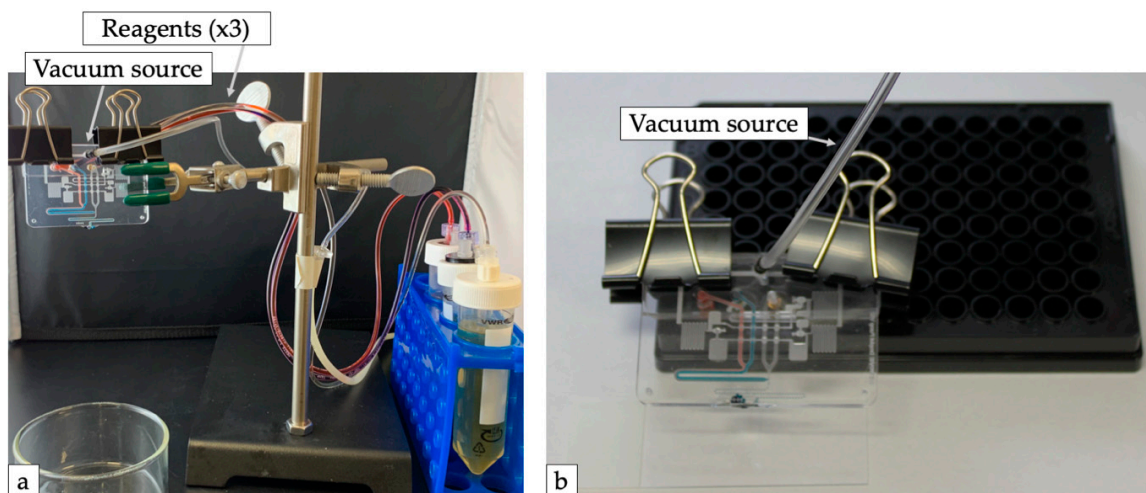
**Figure S4:** Mixing performance was quantified by measuring the distance of the red/blue interface from the center of the channel. When pumps are not synchronized, the flows become unbalanced when vacuum power is increased.



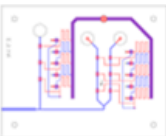
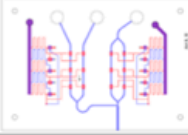
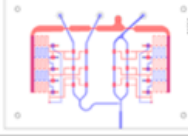
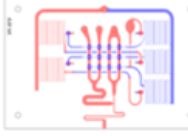
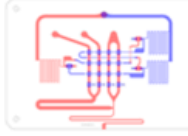
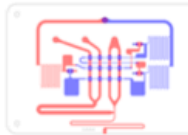
**Figure S5:** Parallel and series pump valve arrangements **(a)** Parallel circuit: The inverter output signal is split to connect both a pump valve and the next inverter **(b)** Series circuit: The inverter output signal is routed through the pump valve to connect to the next inverter.



**Figure S6:** Valve volume measurement. The volume of water displaced by a single valve was measured for a shallow valve (150 µm, blue) and a deep valve (450 µm, red). The behavior of both valves is similar at low pressures. At higher pressures, shallow valves (blue) become limited by the depth of the displacement chamber and approach the maximum volume of the chamber at around 50 kPa, while deep valves (red) continue to displace more volume as actuation vacuum increases. The maximum volumes were calculated assuming the elastomeric membrane fully conforms to the walls of the valve.



**Figure S7:** Photos of compact experimental setup **(a)** The droplet system requires only a vacuum source and connections to reagents. **(b)** Using short lengths of tubing, droplets are generated directly from the wells of a 96 well plate.

Ver	Drawing	Changes	Results	Hypothesis
2		Initial design: One oscillator drives two pumps to mix liquids. This design produces drops of mixed liquid, not droplets.	Pumps produced unequal flow rates, with the pump farthest from oscillator pumping too slowly.	Compressible flow causing pump valves further from the oscillator to displace less volume.
4		Added additional oscillator to balance pump flow rates. Reduced oscillator frequency and pump valve diameter to lower flow rate.	Even mixing was observed, but smaller drop volumes were wanted. A water-in-oil droplet design was investigated.	Adding an oil pump with a T-junction will produce water-in-oil droplets.
6		Added T-junction and additional oscillator pump to make water in oil droplets. Aqueous phase pumps were consolidated to use single oscillator design by equalizing pump valve path lengths.	Droplets were observed, but only when aqueous phase pump flow rate was reduced.	Increasing oil pump flow rate will produce droplets at higher aqueous phase flow rates.
8		Added additional pump to oil phase to increase flow rate. Separated oil and aqueous pump vacuum supply lines to allow independent flow rate control.	Droplets were observed at most flow rates.	Independent flow rate control of aqueous phase and oil phase not necessary with additional oil pump.
14		Connected oscillator power lines together to simplify control. Improved world-to-chip connection by using smaller fittings. Decreased T-junction nozzle width to produce smaller droplets.	Droplet size and uniformity varied if oil and aqueous pumps were not synchronized.	Oil and aqueous pumps must be synchronized to produce uniform droplets.
18		Synchronized pump stages to a single oscillator circuit to improve droplet uniformity. Connected all pump valves except the final pump row in series with the oscillator.	Droplet volume varied with total flow rate. Did not self-prime reliably.	Adding capacitors, check valves, or additional inverter stages will improve pump synchronization.
27		Reduced oscillator to three inverters to reduce the number of forward flow pulses per cycle from 3 to 2 and decrease total flow rate. Connected final pump row in series with the oscillator. Added check valves to all pump outputs.	Weak aqueous phase pumps. The right aqueous phase pump overpowered the left pump at higher input pressures.	Compressible flow still causing delays between pumps in parallel. Slowing pump waveform will improve valve synchronization and pump uniformity.
32		Removed check valves. Adjusted valve opening and closing times with large capacitors in series before and after all pump stages. Reduced depth of pump valve displacement chambers. Moved pneumatic and liquid connectors to opposite sides to simplify operation.	All pumps prime evenly, uniform-sized droplets produced at all flow rates.	-

**Table S1:** A selection of design revisions illustrate the progression of the optimization process. Channels on the top and bottom layers of the chip are shown in blue and red, respectively. The results of each design revision were used to drive incremental changes in the next revision. Scale Bar = 3 mm.

**Video S1:** Steady state droplet generation from 50 kPa constant vacuum source. The oscillator pump droplet system is connected to an electric vacuum pump via a vacuum regulator set to 50 kPa. 21  $\mu$ L droplets are produced at a rate of 2.2 Hz with a 1.1% CV. The video is presented in real time.

**Video S2:** Electricity free droplet generation. A 60 mL locking syringe is directly connected to the oscillator pump droplet system. The plunger is pulled and locked at the 60 mL mark, generating approximately 90 kPa of vacuum pressure that gradually decreases as the droplet pump operates. The system runs for over 14 minutes from this vacuum supply, producing 465 droplets. The video is presented in real time.

**Video S3:** Oscillator pump droplet generator response time. A 70 kPa constant vacuum source is connected to the oscillator pump droplet system and switched on and off via an external solenoid valve. The system responds almost instantly and resumes steady state droplet generation after expelling liquid remaining in the T-junction from the previous operation. The video is presented in real time.

### Calculation S1: Hydraulic Resistance

The hydraulic resistance of a rectangular and square microchannels were calculated using the equations S1 and S2.<sup>37</sup>

$$R_{h,rect} \cong \frac{12 \mu L}{(w h^3)(1 - (0.630 h))} \quad (S1)$$

$$R_{h,square} \cong \frac{28.4 \mu L}{h^4} \quad (S2)$$

Where L, w, h are the channel dimensions and  $\mu = 18.13 \mu Pa * s$ , dynamic viscosity of air at 20°C.<sup>38</sup>

Resistor channels: (200  $\mu m \times 100 \mu m$ ):  $R_h \cong 1.6 \frac{g}{mm^5 s}$  per mm

Interconnect channels: (400  $\mu m \times 400 \mu m$ ):  $R_h \cong 2.0 * 10^{-2} \frac{g}{mm^5 s}$  per mm

Power bus channels: (1000  $\mu m \times 1000 \mu m$ ):  $R_h \cong 5.1 * 10^{-4} \frac{g}{mm^5 s}$  per mm

### Calculation S2: Capillary Number

The capillary number for the continuous phase was calculated using equation S3<sup>39</sup>

$$Ca = \frac{\mu_c v_c}{\gamma} \quad (S3)$$

where  $\mu_c = 33 mPa * s$  is the dynamic viscosity of the continuous phase,<sup>40</sup>  $v_c$  is the mean speed of the continuous as phase extracted from video, and  $\gamma = 24.8 \frac{dyn}{cm}$  is the interfacial tension between the continuous and disperse phases.<sup>41</sup>